Differential Tsunami Travel Time Modeling

The tsunami arrivals from the Mw 8.6 and Mw 8.2 earthquakes are picked on water-level records after tidal effects are removed. Often, coastal stations are noisy, making the tsunami picks difficult. In order to incorporate this uncertainty in the picked time, a range is chosen, i.e., the earlier possible arrival and latest possible arrival, as well as the most likely arrival time. These measurements are differenced (Mw 8.6 observation − Mw 8.2 observation) to derive a differential travel time. We also correct for the time difference between the hypocentral times of the two events. The resulting differential travel times, with respect to the station azimuth calculated at the epicenter of the Mw 8.6 earthquake, are shown in Figure 3B.

The differential travel time approach is often used in seismology to empirically remove path-specific perturbations such as effects due to long-wavelength velocity structure and local effects near the station. For tsunami modeling, the differential travel time approach allows us to make corrections due to effects of dispersion (deep water effects) while incorporating variable seafloor bathymetry that can be calculated with the shallow-water approximation. Specifically, dispersion, in addition to making waves at different frequency travel with different speeds, makes long-wavelength waves arrive earlier than expected from the shallow-water approximation (DeDontney and Rice, 2011). The magnitude of the perturbation in the travel time due to dispersion is strongly dependent on distance, hence differencing two arrival times from two closely-spaced sources removes most of this unwanted signal. Dispersion should also occur between the two sources, but for events that are relatively nearby, this effect should be small. In addition to the dispersion effect, predicted tsunami travel times are based upon gridded bathymetry. For coastal stations, complex local bathymetry that is not included in the travel time calculations may perturb the wave arrival time significantly.

The differential travel time observations provide information about relative locations of the two sources considered. Zero differential travel time indicates that the two sources are co-located. If it is negative, the first (Mw 8.6) source is located closer to the station than the second (Mw 8.2) source, and vice versa. Figure 3(B) shows that the differential travel times show consistency between stations at similar azimuths, demonstrating the robustness of this data set. In contrast, if individual absolute travel times are compared, the data show large scatter. However, the differential travel time information is relative, i.e., we need additional information/assumptions before the source can be mapped. We take the smaller of the two earthquakes (Mw 8.2), and use its epicentral location as the reference point, or where the tsunami associated with this earthquake originated. Considering that the Mw 8.2 earthquake does not have much spatial extent based upon the back-projection study, the assumption of tsunami generation at the epicentral location should be reasonable. The results presented in Figure 2(B) do not change significantly if the reference point is moved slightly to the north or south of the Mw 8.2 epicenter.

Once the reference location is defined, differential travel times can be modeled with respect to this physical point. However, in order to convert time information to space information, we need inverse tsunami travel times from each station. For this purpose, we calculate inverse tsunami travel times for each station, i.e., using the station location as the tsunami source and determine tsunami travel times on a 10-minute grid. In some cases, nearest grid point to the station is located on land or in too shallow water to initiate the travel time calculation. The next

closest suitable grid point is used for these stations. Once inverse travel times are obtained, the travel time at the reference point is subtracted to produce the needed relationship between differential travel time and location.

Before modeling the source location, one final uncertainty we include in our analysis is the effect associated with source duration. We make the assumption that the tsunami waves are generated coseismically, but giant earthquakes can take a long time to complete (e.g., 2004 Sumatra-Andaman earthquake lasts for 9 minutes). A tsunami wave can be generated at the beginning or the end of the rupture, hence the travel time is any time between the picked time with respect to the hypocentral time or the picked time with respect to the end of the rupture. When this effect is incorporated, the observed differential ranges between Δ_s and Δ_e, where these two parameters include source durations of the two earthquakes being considered. In addition, we have picking uncertainty for each tsunami arrival that introduces two more ranges, $d\Delta^-$ and $d\Delta^+$ for earlier and later times. So the differential travel time being modeled is somewhere between $\Delta_s - d\Delta^-$ and $\Delta_e + d\Delta^+$. In this study, we use source durations of 180 and 80 seconds for the Mw 8.6 and 8.2 events, respectively, values that have been obtained from the back-projection analysis.

Using this time range for each station, a sensitivity or likelihood function of the source location is defined. At a given grid location j with the predicted differential travel time t_j, the source sensitivity is defined as

$$g(t_j) = \begin{cases} 1.0 \quad \text{for} \quad \Delta_s \le t_j \le \Delta_e \\ \frac{1}{2}\left[\cos\left(\frac{t_j}{d\Delta^-}\pi\right) + 1.0\right] \quad \text{for} \quad \Delta_s - d\Delta^- \le t_j < \Delta_s \\ \frac{1}{2}\left[\cos\left(\frac{t_j}{d\Delta^+}\pi\right) + 1.0\right] \quad \text{for} \quad \Delta_e < t_j \le \Delta_e + d\Delta^+ \\ 0.0 \quad \text{for} \quad t_j \le \Delta_s - d\Delta^- \quad \text{or} \quad t_j \ge \Delta_e + d\Delta^+ \end{cases}$$

This function assigns a value of 1.0 at locations that are within uncertainty due to source duration, and 0.0 for locations that are outside of the range of differential travel time including picking uncertainties. Between these locations, the sensitivity decays from 1.0 to 0.0 as a cosine function and the width is determined by how well each tsunami arrival can be identified (Figure DR1). Once the sensitivity function is obtained over the source region for all stations, they are summed to determine the source location (Figure 2B).

Figure DR1: The sensitivity function for the Hanimaadhoo station.

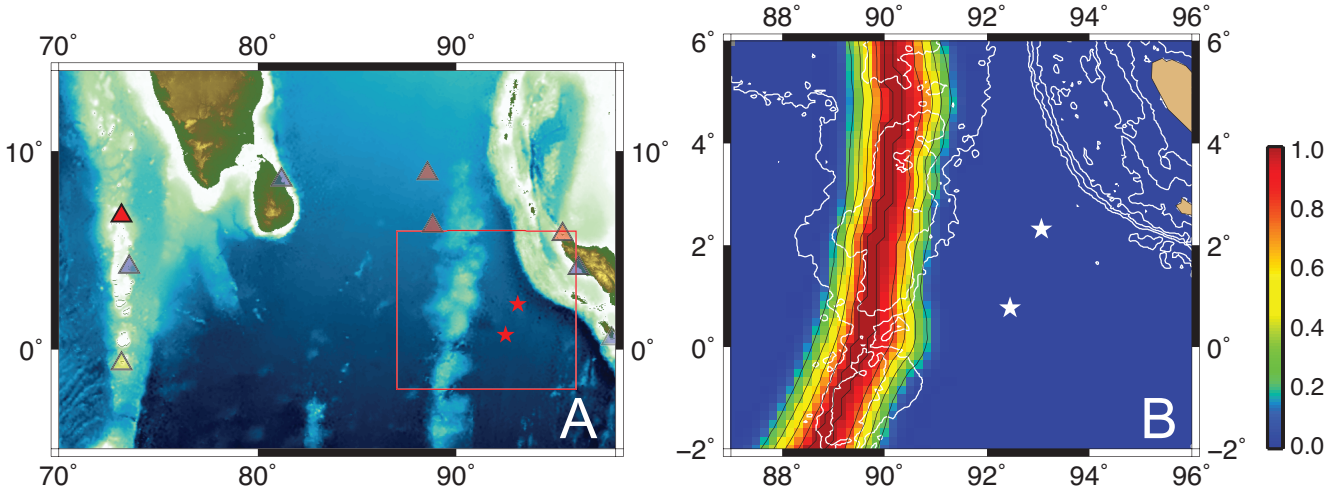

(A) Location of the Hanimaadhoo station in the Indian Ocean (red triangle with black outline). The other transparent triangles show some of the water-level observatory locations with the same color assignment as in Figure 1B. The two red stars denote the epicenters of the Mw 8.6 and 8.2 earthquakes (U.S. Geological Survey, 2012), and the background color shows bathymetry and topography (National Geophysical Data Center, 2006). The region shown in (B) is outlined with a red box.

(B) Sensitivity function $g(t_j)$ for the Hanimaadhoo station. The first tsunami arrival from the Mw 8.6 earthquake is from somewhere along the Ninety-East Ridge, and cannot be from a source near the epicenters of the two earthquakes (white stars). The white contours show seafloor bathymetry (National Geophysical Data Center, 2006). Using a higher resolution bathymetric grid will introduce more structure to the shape of the sensitivity function, but this effect is small compared to uncertainty in picking the tsunami arrival time.